Journal of Physics: Conference Series **712** (2016) 012141 doi:10.1088/1742-6596/712/1/012141

New data evaluation procedure including advanced background subtraction for radiography using the example of insect mandibles

Stefan Mangold*[1], Thomas van de Kamp[2,3], Ralph Steininger[1]

[1] Karlsruhe Institute of Technology, ANKA/IBPT (KIT), P.O. Box 3640, D-76021 Karlsruhe, Germany
[2] Karlsruhe Institute of Technology, Institute for Photon Science and Synchrotron Radiation (KIT-ANKA-IPS), P.O. Box 3640, D-76021 Karlsruhe, Germany
[3]Karlsruhe Institute of Technology, Laboratory for Applications of Synchrotron Radiation, P.O. Box 3640, D-76021 Karlsruhe, Germany

E-mail: stefan.mangold@kit.edu

Abstract. *The usefulness of full field transmission spectroscopy is shown using the example of mandible of the stick insect Peruphasma schultei. An advanced data evaluation tool chain with an energy drift correction and highly reproducible automatic background correction is presented. The results show significant difference between the top and the bottom of the mandible of an adult stick insect.*

1. Introduction

The usefulness of full field transmission spectroscopy can be attributed to the fact that spectral information is collected in parallel, thus avoiding the time-consuming scanning of the sample through a micro-focussed X-ray beam. Therefore this technique is more and more used to gain insight into complex and large sample systems in catalysis, environmental science and biology. Pioneering work in X-ray Absorption Near Edge Structure (XANES) imaging of catalyst has been reported in [1]. During this work a correction of the (vertical) energy drift over the detector and a background subtraction of the spectra were omitted. A formula to calculate the energy drift dependent on the divergence of the x-ray beam and type of crystal in the monochromator is described here [2]. A significantly enhanced data evaluation chain was presented in combination with measurements of an x-radia microscope set-up here [3]. Because this group still omitted the energy calibration/inspection and used a very simple background subtraction, we aimed to develop our own data evaluation chain.

Zinc plays a critical role in the mechanical properties of invertebrate jaws and mandibles [4]. The zinc species distribution is important to understand the exceptional high hardness and Young's modulus. Volume renderings of the head of the stick insect Peruphasma schultei [5] based on tomographic white beam measurements showed the suitability of this mandibles for full field XANES measurements [6]. A large and homogenous beam is needed to take full advantage of the large available detector area. As a bulk bending magnet beamline, ANKA-XAS is therefore very well suited. Due to the absence of any focusing mirrors the beamline delivers a beam of very uniform intensity across 11 x 1 mm^2 and is therefore well-suited for radiography of laterally extended samples.

2. Experimental

The difference to the standard XAFS set-up was the installation of the camera set-up between **M-850.50** Hexapod 6 Axis micro positioning system from PI and the second ionisation chamber. The high-resolution X-ray imaging detector system consists of a YAG fluorescence screen a vertical reflecting mirror, Mitutoyu long working distance microscope objective and a PCO-edge camera [7]. The effective pixel size on the sample is 5 by 5 μm^2 and therefore the set-up generates more than 500.000 Absorption Near Edge Structure (XANES) data sets in each radiogram. Even with the reduction of the measurement time per point by a factor of 10 to earlier measurements this systems offers a dramatically improved signal to noise ratio. Since a full field XANES measurement relies on a significant absorption jump per pixel or voxel (tomographic measurements) and therefore many samples have to be thicker than 50 μm in the medium X-ray energy range, the setup uses a flux-optimized optic with a well suitable lateral resolution of 5 μm.

3. Data evaluation

The image data are cached on advanced RAID-0 system and uploaded regular to a data cruncher with RAID5 data storages connected by Thunderbolt (MacPro, 1Gb/s SSD, 64 Gb RAM, 600 Mb/s read/write on storages). The single steps of the advanced data evaluation tool chain based on IgorPro [8] are described in table 1. Similar data evaluation procedures have been reported by other groups [9].

Table 1: Data evaluation steps

Data evaluation step	Description	Time needed per core (standard intel CPU)
Calculation of spectra	Calculation of spectra by ln(measurement without sample/ measurement with sample) for each detector pixel (ln = natural logarithm)	< 6 min per 4Gb
Calculation of the vertical energy shift	Used for correction of the vertical energy drift over the image	5h (500.000 spectra); only once per edge / core
Correction of the vertical energy shift	Used to correct the beamline dependent vertical energy shift	< 3 min (500.000 spectra)
Edge filtering	Filter out all pixels, which contains no reasonable spectrum	< 2min
Background subtraction	Independent background subtraction for each raw XAFS spectra in each pixel	~100 spectra / core / s
PCA analysis	Detection of components (PCA = principal component analysis)	10s - 15 min
Linear combination	Calculate the loadings of the different components	10 min – 2h / core

Unique steps of this data evaluation are the correction of the small but notable energy drift over the detector due to the illumination of the flat monochromator crystal with a divergent beam and the highly reproducible automatic background correction. The energy correction is done by a measurement of the respective metal foil (or homogenous sample), the fit of the energy-position and a scaling factor of the spectrum in each pixel and the usage of this shift values for each sample data set. The latter obtains its stability due a combination of a sigmoidal fit and a long distance pre- and post-edge fit. Due to this mechanism it can operate also at very low edge jumps down to 0.05. Because the fits are based on highly optimized C-code within IgorPro math libraries, it enables near real time data evaluation. The planned parallelisation of the code will enable faster data evaluation than acquisition. The energy correction and the background subtraction are needed to ensure, that the input data for the PCA contains only background subtracted, normalised data with reasonable edge jump. Without the clean-up steps, the PCA would be overrun by not useful information.

4. Results

Figure 1 shows the transmission image of the sample and differences between the absorption below and above the Zn absorption edge. Parts of the mandible of the stick insect *Peruphasma schultei* inherits an edge jump of nearly 1. This step is used to find area of interest. While the edge jump on the mandibles of the youngest insects is in the range of 0.20 (figure 3 A) and rather constant, the older insects have a significant stronger absorption on the tip of the mandible.

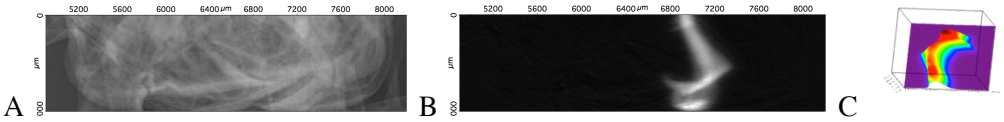

Figure 1. A) Transmission image of the sample; B) difference between after and before absorption edge. C) Zinc concentration over sample area, all plots show the mandible of an adult insect

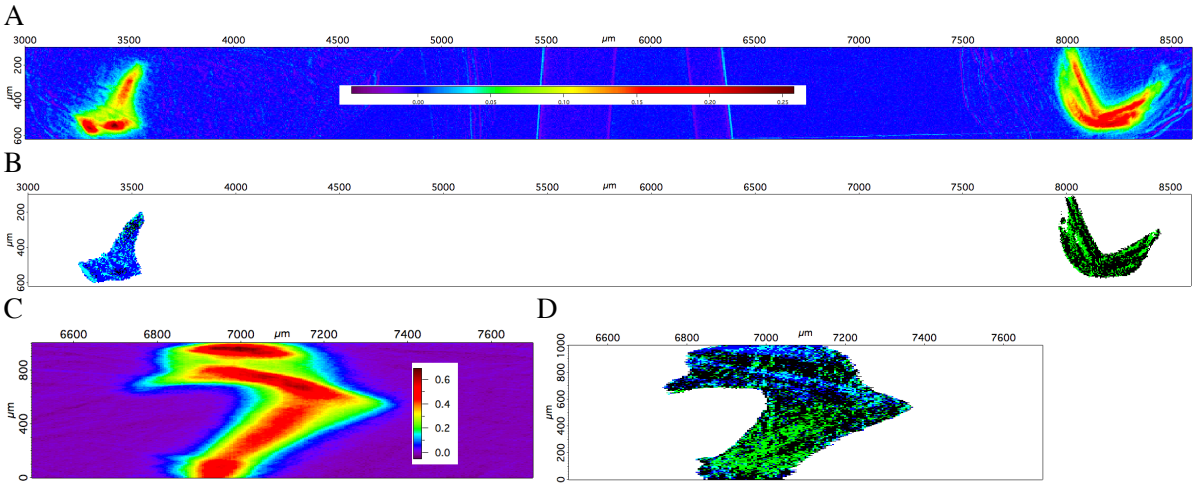

Figure 2. A) Absorption image plot shows the difference between after and before absorption edge. **B)** Distribution of the 3 PCA components over the mandibles, right side shows a young hatchling (larval stage 1) before it started feeding, left side an older larva of the same stage. C) Absorption image plot of the mandible of adult insect (difference between after and before absorption edge). D) Distribution of the 3 PCA components over the same mandible

Figure 2A illustrates the results of the linear combination fit of the 3 PCA-components over the mandibles in the youngest stick insects. There is a significant difference between the right (hatchling before it started feeding) and left mandible, but no remarkable difference over the mandible itself. The absorption for the mandibles of the adult insect at the zinc edge is larger than the juvenile ones (2C). The difference of the extracted PCA components are also significantly larger. While there is only a small change between inner and outer exoskeleton, there are significant differences between basis (bottom) and cutting edge (top) of the mandible.

The spectra presented in figure 3 indicate the small but distinct difference over the height of the mandible of an adult insect, which should be responsible for different hardness of the structures. The difference also between the mandibles of the younger insects (hatchling and older larval stage 1) is even smaller (figure 3). First literature studies indicate the presences of two different types of zinc-proteins [10]. Two mixtures (75/60 % and 25/40 %) of zinc-histidine and zinc cysteine are added to the plots for comparison.

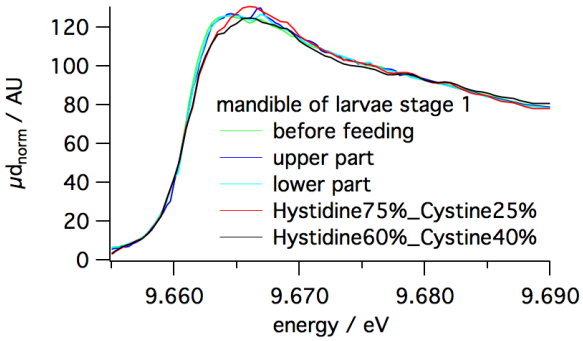

Figure 3. Distribution of the 3 PCA components over the mandible of hatchling and older larval stage 1

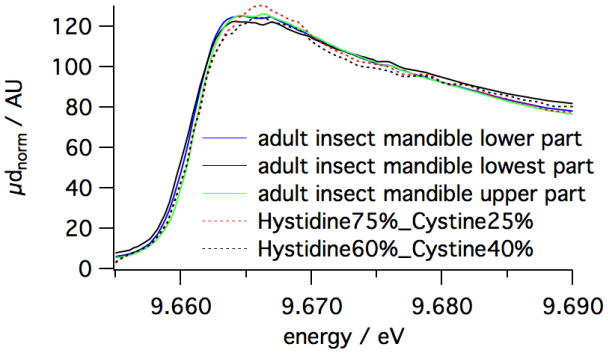

Figure 4. Distribution of the 3 PCA components over the mandible of the adult insect.

5. Conclusion

The improvement of the signal to noise ratio of the measurement and the improved data reduction tool chain shows the progress of a prototype experiment to a reliable analytical tool, which can be used for a large set of different sample like batteries, catalytic systems, art and mineral samples. The quality of the data evaluation is needed to detect the small difference between species in the mandibles. With the growth of the insect also the distribution of the species is changing.

Acknowledgement

We acknowledge the Synchrotron Light Source ANKA for provision of beamtime.

References

[1] Grunwaldt J-D, Hannemann S, Schroer C G and Baiker A 2006 *J. Phys. Chem.* B **110** 8674-8680
[2] Katayama M, Sumiwaka K, Hayashi K, Ozutsumi K, Otha T and Inada Y 2012 *J. Synchrotron Rad.* **19** 717–721
[3] Meirer F, Cabana J, Liu Y, Mehta A, Andrews J C and Pianettac P 2011 *J. Synchrotron Rad.* **18** 773–781
[4] Broomell C C, Mattoni M A, Zok F W and Waite J H 2006 *J. Exp. Biol.* **209** 3219-3225
[5] Conle O V and Hennemann F H 2005 *Zootaxa* **1068** 59-68
[6] Van de Kamp T, Ershov A, Dos Santos Rolo T, Riedel A and Baumbach T 2013 *Entomologie heute* **25** 147-160
[7] Cecilia A, Rack A, Douissard P A, Martin T, dos Santos Rolo T, Vagovič P, Hamann E, van de Kamp T, Riedel A, Fiederle M and Baumbach T 2011 *Nucl. Instr. Methods. A* **648** Supplement 1 321-323
[8] IgorPro - http://www.wavemetrics.com/ 10.10.2015
[9] Liu Y, Meirer F, Williams P A, Wang J, Andrews J C and Pianetta P 2012, J. Synchrotron Rad. **19** 281-287
[10] Terzano R, Chami Z A, Vekemans B, Janssens K, Miano T and Ruggiero P 2008, *J. Agric. Food Chem.* **56** 3222–3231